

Resonant collisional dissociation of Na_2^+ by $\text{Na}(3p)$ in an effusive beam

Charles Tapalian and Winthrop W. Smith

Physics Department, University of Connecticut, Storrs, Connecticut 06269

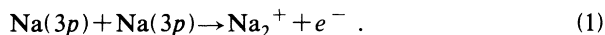
(Received 13 September 1993)

We observe the production of Na^+ ions in a single effusive sodium atomic beam via intrabeam dissociating collisions of laser-excited $\text{Na}(3p)$ atoms with Na_2^+ ions created by associative ionization. The rather large cross section for this collisional dissociation process has been experimentally determined to be $3(\pm 1) \times 10^{-13} \text{ cm}^2$ at a source temperature of $\approx 530 \text{ K}$. A classical Langevin model gives an estimate based on long-range forces of about twice this value.

PACS number(s): 34.50.Lf, 34.50.Rk, 33.80.Gj, 34.20.Gj

I. INTRODUCTION

In the course of studying effusive beams of laser-excited alkali atoms, associative ionization (AI) has been a topic for much investigation. An effusive (500–600 K) beam of sodium atoms can be excited from the $3s$ electronic energy level to the $3p$ electronic energy level by absorption of 589-nm light. The exothermic AI reaction for the $\text{Na}(3p)$ excited sodium atoms is a collision of two $\text{Na}(3p)$ atoms resulting in a Na_2^+ molecular ion in a low-lying vibrational state and an electron:



Collision cross sections for this reaction have been obtained under various conditions by many experimental groups [1–4].

This experiment is a study of Na^+ atomic ion production in a single effusive atomic beam of sodium. Our first study of the AI process [5] revealed persistent production of Na^+ ions in addition to the expected Na_2^+ ions which result from AI. The reaction process determined to be responsible for Na^+ ion production is the collisional dissociation of the Na_2^+ ions:

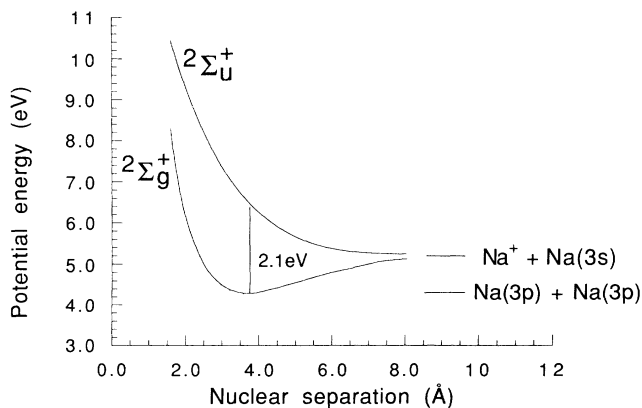
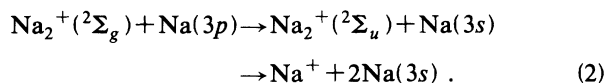


FIG. 1. Na_2^+ molecular potential curves.

The collisional energy transfer of 2.1 eV from $\text{Na}(3p)$ to Na_2^+ , as indicated on the Na_2^+ potential curves in Fig. 1, results in a near-resonant Franck-Condon transition. Identification of reaction (2) is accomplished by analyzing ion yields, obtained using time-of-flight (TOF) mass spectrometry, as functions of atomic sodium density and laser intensity. A related heteronuclear study involving the interaction of a laser-excited atomic beam of cesium in a high Rydberg state with an atomic beam of sodium was published recently by Gabbanini *et al.* [6]. In that study, Cs^+ atomic production resulted from a collision of a cesium Rydberg atom with a ground-state sodium atom.

II. EXPERIMENTAL METHOD

Figure 2 shows the interaction region of the atoms and laser beams. The effusive (subsonic) sodium source oven consists of two stages; a heated cylindrical reservoir and a 3-in.-long nozzle with a $\frac{1}{16}$ -in.-diam, 1-in.-long heated channel from which the atoms effuse. The lasers are focused close to the nozzle aperture in order to sample a region of high sodium density (densities of $\sim 10^{12}$ atoms/cm³ are common). Product ions are extracted

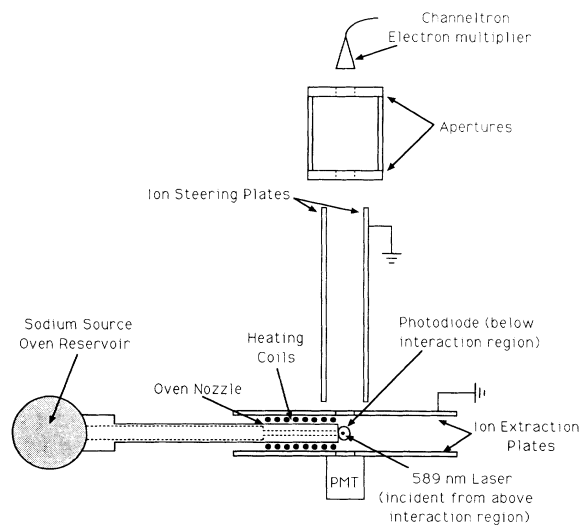


FIG. 2. Schematic diagram of time-of-flight atomic beam apparatus.

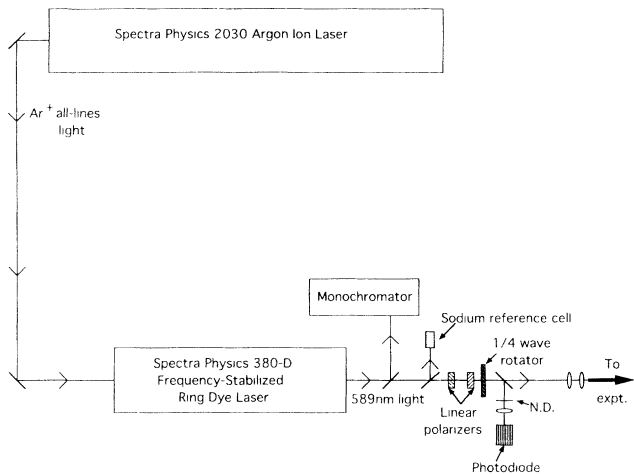


FIG. 3. Lasers and optical components. N.D. denotes a neutral-density filter.

periodically from the interaction region by an electric-field pulse of approximately 50 V/cm and collected within a channel electron multiplier after passing through a short time-of-flight mass analyzer perpendicular to the atomic beam.

Figure 3 shows the lasers and associated optical components used in the experiment. A cw, circularly polarized, frequency-stabilized, narrow-band (~ 1 MHz) dye laser is tuned to 589 nm to excite the Na $3s$ ($^2S_{1/2}$) to Na $3p$ ($^2P_{3/2}$) D_2 electronic transition of sodium. Laser intensities of up to 100 W/cm^2 incident on the atoms are attainable, well above the Doppler-broadened atomic saturation intensity. Measurements of ions and fluorescence as functions of laser intensity provide saturation curves from which the effective relative saturation intensity and other parameters required to determine the cross sections are extracted.

The atomic sodium density is determined by measuring the fraction of light transmitted through the atomic beam. To obtain an accurate density measurement, the dye-laser intensity must be much less than the saturation intensity for the D_2 transition. The density is then calculated using the formula

$$\sigma n_0 L = -\ln(I/I_0), \quad (3)$$

where σ is the Doppler-broadened absorption cross section, n_0 is the total atomic sodium density, L is the absorption length, and I/I_0 is the transmitted fraction of light.

III. LANGEVIN MODEL

We have modeled the resonant collisional dissociation process, Eq. (2), in a very simple way as a classical Langevin cross section [7]. Na_2^+ ions are formed in the effective beam by collisions of laser-excited Na($3p$) atoms. The electric field of one of these ions then polarizes a neighboring laser-excited Na($3p$) atom in the beam via the long-range attractive potential (in atomic units)

$$V(r) = -\frac{1}{2} \frac{\alpha_{3p}}{r^4}, \quad (4)$$

where α_{3p} is taken as the scalar polarizability of the target Na($3p$) atom. The excited-state Na($3p$) polarizability is somewhat enhanced (by a factor ~ 3) relative to that of the Na($3s$) ground state [8]. This strong, long-range attraction “harpoons” the Na($3p$) atom which then reacts with the Na_2^+ ion, dissociating it into $\text{Na}^+ + \text{Na}(3s)$. We now look at the collision dynamics in more detail.

Figure 4 shows an example of the *classical deflection function* $\Theta(b)$ for potential scattering of thermal-energy sodium atoms by Na_2^+ ions using the long-range potential of Eq. (4). The incident c.m. frame kinetic energy is assumed to be characteristic of a thermal beam in the 500–600-K range. At a specified c.m. energy

$$E = \frac{1}{2} \mu v_{\text{CD}}^2, \quad (5)$$

where μ is the reduced mass and v_{CD} the relative velocity of the two colliding partners (CD denotes collisional dissociation), there is a range of impact parameters b which gives large (negative) scattering angles in excess of 180° . *Orbiting* of the projectile around the target thus occurs and the interaction time of the collision is much greater than that for a single-pass collision. We then assume that under these conditions the probability of a collisional dissociation reaction approaches 100%, without specifying the mechanism in detail. This is particularly plausible for the special case of sodium, where the excitation transfer from the Na($3p$) to the Na_2^+ is *near resonant*.

Figure 5 shows another way to look at this situation: via the effective one-dimensional potential for the relative radial motion in the collision [9], including the angular momentum barrier. This effective potential has the form (in atomic units)

$$V_{\text{eff}}(r) = -\frac{1}{2} \frac{\alpha_{3p}}{r^4} + E \frac{b^2}{r^2}, \quad (6)$$

where E is the c.m. frame kinetic energy and b is the impact parameter. The barrier height is given by

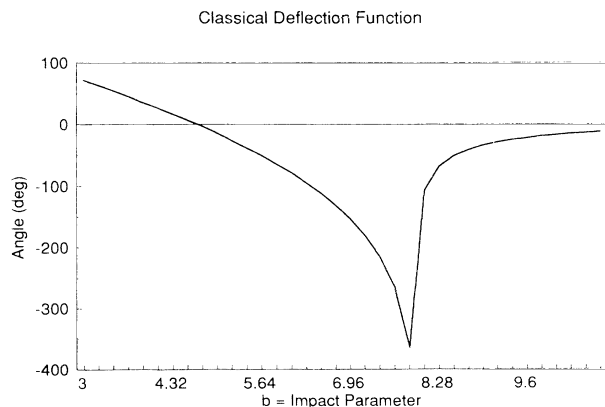


FIG. 4. Example of the classical deflection function for the scattering angle $\Theta(b)$ in a hypothetical model potential which includes a short-range repulsion between the atomic and molecular cores plus a $1/r^4$ long-range attraction. Typically, orbiting occurs in a narrow range of impact parameters b (atomic units), but smaller b values also lead to long interaction times at close range.

$$V_{\max} = \frac{1}{2} E^2 \frac{b^4}{\alpha_{3p}}, \quad (7)$$

with the barrier maximum located at

$$r_{\max} = \frac{\left[\frac{\alpha_{3p}}{E} \right]^{1/2}}{b}; \quad (8)$$

note that V_{\max} increases with increasing b . In classical scattering (de Broglie wavelength $\ll r_{\max}$), the reaction can occur ($r \rightarrow 0$ during the collision) only when the c.m. kinetic energy $E > V_{\max}$. The condition $E = V_{\max}$ then leads to a maximum impact parameter b_{\max} , such that the projectile and target can approach each other closely enough for the collisional dissociation reaction to occur:

$$b_{\max}^2 = \left[\frac{2\alpha_{3p}}{E} \right]^{1/2}. \quad (9)$$

For $b < b_{\max}$, the barrier is lower and the reactants can approach closely. If we assume the reaction probability is 100% if the particles approach each other within the

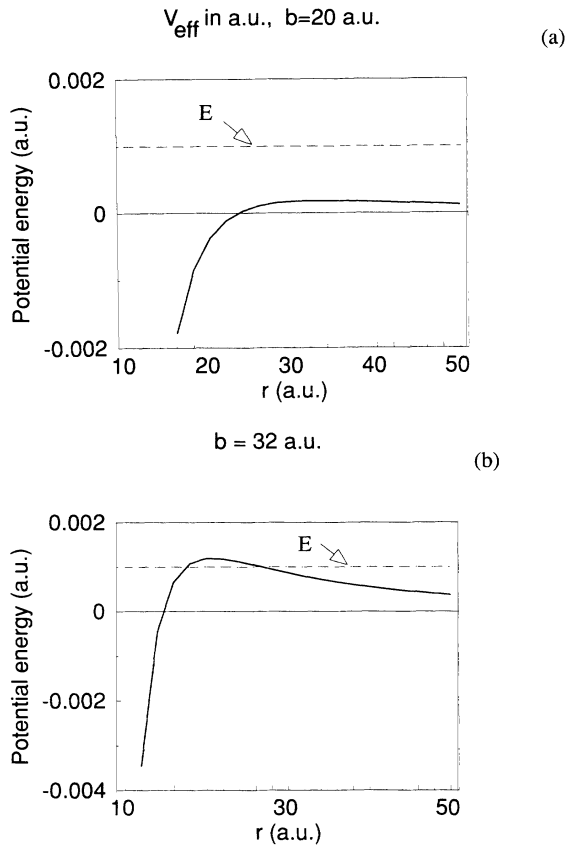


FIG. 5. Effective one-dimensional model potential for the radial motion in a molecular-ion-excited atom collision: $V_{\text{eff}}(r) = -\frac{1}{2}(\alpha_{3p}/r^4) + E(b^2/r^2)$, where E is the c.m. collision energy and b is the impact parameter (in atomic units). Here E is set at 0.001 a.u. as a typical value, and α_{3p} is the $\text{Na}(3p)$ polarizability. (a) $b = 20$ a.u. (Bohr radii); (b) $b = 32$ a.u. Note that in (b) with $b_{\max} > E$, a close (reactive) interaction is prevented by the barrier.

barrier ($r < r_{\max}$) rather than being reflected from the barrier, the estimated cross section becomes πb_{\max}^2 . This, in addition to Eqs. (5) and (9), leads to a collisional dissociation cross section given by

$$\sigma_{\text{CD}} = \pi b_{\max}^2 = \pi \left[\frac{2\alpha_{3p}}{E} \right]^{1/2} = 2\pi \left[\frac{\alpha_{3p}}{\mu v_{\text{CD}}^2} \right]^{1/2}. \quad (10)$$

Looking now at the *rate coefficient* k_{CD} for the collisional dissociation reaction, $k_{\text{CD}} = \sigma_{\text{CD}} v_{\text{CD}}$, implying an average over the distribution of relative velocities in the beam, and using Eq. (10) we find

$$k_{\text{CD}} = \overline{\sigma_{\text{CD}} v_{\text{CD}}} = 2\pi \left[\frac{\alpha_{3p}}{\mu} \right]^{1/2}, \quad (11)$$

in atomic units (a.u.), independent of v_{CD} . This is a characteristic of the r^{-4} long-range interaction potential. Thus the rate coefficient k_{CD} will be independent of velocity as long as the above assumptions are valid, including the classical treatment of the collisions. For very cold collisions, quantum effects will need to be considered, but the classical approach taken here (de Broglie scattering wavelength $\ll r_{\max}$) appears to be valid for beam temperatures in the 500–600-K range of these experiments.

Substituting values for the parameters in Eq. (11), we obtain the following estimated maximum value for the rate coefficient from this collision model: $k_{\text{CD}} = 30.3$ a.u. $= 1.9 \times 10^{-7}$ cm³/sec. An approximate estimate of the velocity averaged collisional dissociation cross section is obtained using the expression for the relative collision velocity v_{CD} [10,11] in the beam,

$$\overline{v_{\text{CD}}} = \frac{(7 - 4\sqrt{2})}{\sqrt{2\pi}} v_0, \quad (12)$$

where $v_0 = \sqrt{2kT/m}$ is the most probable atomic velocity in the source. At an average source temperature of 530 K, $\overline{v_{\text{CD}}} \approx 3.3 \times 10^4$ cm/sec, and $k_{\text{CD,max}} \approx \sigma_{\text{CD,max}} \overline{v_{\text{CD}}}$, therefore $\sigma_{\text{CD,max}} \approx 5.6 \times 10^{-12}$ cm². These theoretically predicted values from the Langevin model are compared with the experimentally measured values in a later section.

IV. RESULTS AND ANALYSIS

A. Reaction process identification

Identification of the reaction processes is accomplished through qualitative analysis of the measured ion yields as functions of atomic density and laser intensity. There are several energetically allowed reaction processes which could result in the formation of Na^+ ions. These include the multiphoton ionization of $\text{Na}(3p)$, collisional dissociation of Na_2^+ , photodissociation of Na_2^+ , photoionization of $\text{Na}(4d,5s)$ excited atoms created by energy pooling [12], and Penning ionization of $\text{Na}(4d,5s)$ created by energy pooling [13]. The photodissociation of Na_2^+ has been studied theoretically [14] and experimentally [15,16] using high-intensity pulsed lasers. In this experiment, however, the cw laser intensities used are too low to account for Na^+ production via this reaction. Multiphoton ionization of $\text{Na}(3p)$ can also be neglected due to low

laser intensities. In order to determine the extent of the energy pooling reaction, a second cw laser, nonresonant with any electronic transitions of sodium, is directed at the sodium atoms. A second tunable dye laser and several Ar⁺ laser lines are utilized for this purpose. If a significant number of Na(4*d*,5*s*) excited atoms are present, an *enhancement* of the Na⁺ ion yield would result due to photoionization. No such Na⁺ *enhancement* is observed. The results of this test also indicate that the photodissociation of Na₂⁺ can be neglected since the resultant Na⁺ ion yield would be dependent on the intensity of the second laser. Collisional dissociation of Na₂⁺ thus seems to be the only remaining possibility for Na⁺ formation.

Measurements of Na⁺ ion yield as a function of atomic sodium density indicate a *cubic* dependence (Fig. 6), implying the occurrence of a three-body reaction. The only three-body reactions which could result in Na⁺ formation are the collisional dissociation of Na₂⁺ and the Penning ionization collision of Na(3*p*) with Na(4*d*,5*s*) created by energy pooling. Note that the combined excitation energy of two Na(3*p*) atoms is well below the 5.1-eV excitation threshold for direct Penning ionization. A second tunable dye laser tuned to the Na(3*p*)→Na(4*d*) electronic transition of sodium is used to observe ionization of Na(4*d*) excited atoms. The measured Na⁺ ion yield resulting from Na(4*d*) is determined to be a linear function of sodium density indicating that these Na⁺ ions are produced primarily by the photoionization of Na(4*d*) rather than by the Penning ionization reaction. Therefore from the measurements of the Na⁺ ion yield as a function of sodium density, the collisional dissociation of Na₂⁺ is once again the only remaining possibility.

B. Cross-section determination

An ion production rate equation approach is taken to determine the collisional dissociation cross section from the measured parameters. The rates of production of the ion densities $n_{\text{Na}_2^+}$ and n_{Na^+} are

$$\frac{dn_{\text{Na}_2^+}}{dt} = \overline{\sigma_{\text{AI}v_{\text{AI}}n_{3p}^2}} - \overline{\sigma_{\text{CD}v_{\text{CD}}n_{3p}n_{\text{Na}_2^+}}, \quad (13)$$

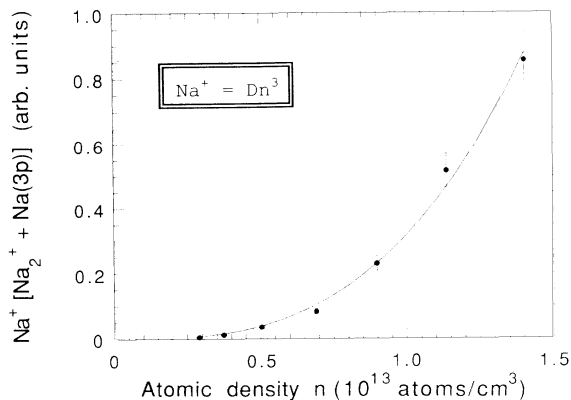


FIG. 6. Na⁺ (collisional dissociation) ion yield vs atomic density.

$$\frac{dn_{\text{Na}^+}}{dt} = \overline{\sigma_{\text{CD}v_{\text{CD}}n_{3p}n_{\text{Na}_2^+}}. \quad (14)$$

The Na₂⁺ rate equation can be integrated over the interaction time T_1 , the amount of time the atoms are within the laser field, to provide an expression for $n_{\text{Na}_2^+}$ as a function of the Na(3*p*) density n_{3p} . Two assumptions are made to simplify this integral: there exists a steady-state Na(3*p*) population ($dn_{3p}/dt=0$), and the rate of production of Na₂⁺ is much larger than the rate of dissociation of Na₂⁺ ($\sigma_{\text{AI}v_{\text{AI}}n_{3p}^2} \gg \sigma_{\text{CD}v_{\text{CD}}n_{3p}n_{\text{Na}_2^+}$).

Thus

$$\frac{dn_{\text{Na}_2^+}}{dt} \simeq \overline{\sigma_{\text{AI}v_{\text{AI}}n_{3p}^2}}, \quad (15)$$

or

$$\Delta n_{\text{Na}_2^+} = \overline{\sigma_{\text{AI}v_{\text{AI}}n_{3p}^2} T_1}. \quad (16)$$

This expression for $\Delta n_{\text{Na}_2^+}$ can be substituted into the rate equation for Na⁺ giving

$$\frac{dn_{\text{Na}^+}}{dt} = \overline{\sigma_{\text{CD}v_{\text{CD}}n_{3p}(\sigma_{\text{AI}v_{\text{AI}}n_{3p}^2} t)}. \quad (17)$$

Integrating this expression over the interaction time T_2 , the amount of time the Na₂⁺ ions are within the laser field, results in

$$\Delta n_{\text{Na}^+} = \frac{1}{2} \overline{\sigma_{\text{CD}v_{\text{CD}}n_{3p}(\sigma_{\text{AI}v_{\text{AI}}n_{3p}^2} T_2^2)}. \quad (18)$$

The rate equation solution for the steady-state Na(3*p*) population is

$$n_{3p} = \frac{I/I_{\text{sat}}}{1 + 2I/I_{\text{sat}}} n_0, \quad (19)$$

where I is the laser intensity, I_{sat} is the effective saturation intensity for the broadened absorption profile, and n_0 is the total atomic density. This solution is valid over the range of laser intensities for which the power-broadened linewidth is much less than the Doppler absorption linewidth at $I \ll I_{\text{sat}}$. Equations (16) and (18) can be expressed as functions of laser intensity using Eq. (19):

$$\Delta n_{\text{Na}_2^+} = \overline{\sigma_{\text{AI}v_{\text{AI}} T_1 n_0^2} \left[\frac{I/I_{\text{sat}}}{1 + 2I/I_{\text{sat}}} \right]^2}, \quad (20)$$

$$\Delta n_{\text{Na}^+} = \frac{1}{2} \overline{\sigma_{\text{CD}v_{\text{CD}} \sigma_{\text{AI}v_{\text{AI}} T_2^2 n_0^3} \left[\frac{I/I_{\text{sat}}}{1 + 2I/I_{\text{sat}}} \right]^3}. \quad (21)$$

In order to obtain expressions for the number of ions produced within the interaction volume, Eqs. (20) and (21) must be integrated over the volume. Using a Gaussian laser beam intensity profile,

$$I = I_0 e^{-2r^2/w^2}, \quad (22)$$

the volume integration results in

$$\Delta N_{\text{Na}_2^+} = \frac{\pi}{8} L w^2 \overline{\sigma_{\text{AI}v_{\text{AI}} T_1 n_0^2 F(I_0/I_{\text{sat}})}, \quad (23)$$

$$\Delta N_{\text{Na}^+} = \frac{\pi}{32} L w^2 \overline{\sigma_{\text{CD}} \nu_{\text{CD}}} \overline{\sigma_{\text{AI}} \nu_{\text{AI}}} T_2^2 n_0^3 G(I_0/I_{\text{sat}}), \quad (24)$$

where

$$F(I_0/I_{\text{sat}}) = \ln(1 + 2I_0/I_{\text{sat}}) - \frac{2I_0/I_{\text{sat}}}{1 + 2I_0/I_{\text{sat}}}, \quad (25)$$

$$G(I_0/I_{\text{sat}}) = \ln(1 + 2I_0/I_{\text{sat}}) - \frac{2I_0/I_{\text{sat}}(1 + 3I_0/I_{\text{sat}})}{(1 + 2I_0/I_{\text{sat}})^2}, \quad (26)$$

L is the atomic beam absorption length, and w is the $1/e^2$ laser spot radius. The expressions (23) and (24) for $\Delta N_{\text{Na}_2^+}$ and ΔN_{Na^+} must each be multiplied by a factor η which includes the detection efficiency and extraction pulse rate in order to be compared with the experimental ion yields. The experimental values of η for Na_2^+ and Na^+ are approximately equal.

Experimental data are acquired by measuring Na_2^+ and Na^+ ion yields as functions of atomic density at constant laser intensity. The Na_2^+ ion yield data are fitted to a quadratic function of density (Fig. 7), $\Delta N_{\text{Na}_2^+} = Cn_0^2$, and the Na^+ ion yield data are fitted to a cubic function of density (Fig. 6), $\text{Na}^+ = Dn_0^3$, where C and D are data fitting parameters. Expressions for C and D in terms of the laser intensity and the cross sections are obtained from Eqs. (23) and (24):

$$C = \frac{\pi}{8} L w^2 \eta \overline{\sigma_{\text{AI}} \nu_{\text{AI}}} T_1 F(I_0/I_{\text{sat}}), \quad (27)$$

$$D = \frac{\pi}{32} L w^2 \eta \overline{\sigma_{\text{CD}} \nu_{\text{CD}}} \overline{\sigma_{\text{AI}} \nu_{\text{SI}}} T_2^2 G(I_0/I_{\text{sat}}). \quad (28)$$

The ratio of the parameters D/C is therefore

$$\frac{D}{C} = \frac{1}{4} \frac{\overline{\sigma_{\text{CD}} \nu_{\text{CD}}}}{\overline{\sigma_{\text{AI}} \nu_{\text{AI}}}} \frac{T_2^2}{T_1} \frac{G(I_0/I_{\text{sat}})}{F(I_0/I_{\text{sat}})}. \quad (29)$$

Values for C and D are obtained from data fitting. The interaction times are approximated from the size of the saturated atom region and the average thermal atomic velocity. In order to determine the ratio of intensity functions $G(I_0/I_{\text{sat}})/F(I_0/I_{\text{sat}})$, the saturation intensity

is obtained experimentally by measuring the ion yields as functions of laser intensity and then data fitting to saturation curves. Using measured values in Eq. (29) yields a result for the collisional dissociation rate coefficient:

$$k_{\text{CD}} = \overline{\sigma_{\text{CD}} \nu_{\text{CD}}} = 1.0(\pm 0.3) \times 10^{-8} \text{ cm}^3/\text{sec}. \quad (30)$$

Using the average relative velocity for this temperature range, $\overline{\nu_{\text{CD}}} \approx 3.3 \times 10^4$ cm/sec, and the approximation $k_{\text{CD}} \approx \overline{\sigma_{\text{CD}} \nu_{\text{CD}}}$, the velocity averaged cross section is $\overline{\sigma_{\text{CD}}} \approx 3(\pm 1) \times 10^{-13}$ cm². The uncertainty in these experimental values is primarily due to statistical fluctuations in the density determination over many sets of data.

V. DISCUSSION

Comparing the values from the Langevin model of Eq. (10), which assumes a transition probability of 100% on every collision having $b < b_{\text{max}}$, we find the experimental rate coefficient k_{CD} , Eq. (30), to be about $\frac{1}{10}$ of $k_{\text{CD,max}}$ from Eq. (11). It is clear, however, from the example of Fig. 4, that the range of *impact parameters* $\Delta b \ll b_{\text{max}}$ should be restricted to large-angle or orbiting collisions having a long interaction time. Then the *upper limits* of Eqs. (10) and (11) should be *reduced* by a factor $\approx \Delta b/b_{\text{max}} \approx 0.1$ [estimated from the range Δb of impact parameters giving a classical deflection function $\Theta(b) \leq -180^\circ$], based on the value of α_{3p} from Ref. [8] and $\overline{\nu_{\text{CD}}} = 3.3 \times 10^4$ cm/sec. This brings the model and experiment for k_{CD} into agreement within a factor of 2, satisfactory considering the simplicity of this modified Langevin model.

The large cross section for collisional dissociation implies this reaction mechanism is very significant in high-density atomic beam experiments. Experiments involving Na_2^+ ions formed by normal associative ionization within an effusive beam could be inhibited by the formation of Na^+ ions due to collisional dissociation. These experiments include, for example, the trapping of Na_2^+ ions formed in a laser-excited beam [17] and the formation of molecular clusters via intrabeam collisions [18]. This process also appears to be relevant to ultracold collisions in ion traps.

VI. SUMMARY

The process responsible for Na^+ ion formation in our cw laser-excited thermal beam experiment has been successfully identified as the resonant, dissociating collision of $\text{Na}(3p)$ excited atoms with Na_2^+ ions. The experimental value obtained for the collisional dissociation cross section is $3(\pm 1) \times 10^{-13}$ cm², while a classical Langevin model based on long-range forces provides an estimate of the collision cross section of $\approx 0.1 \overline{\sigma_{\text{CD,max}}} = 6 \times 10^{-13}$ cm².

ACKNOWLEDGMENTS

We acknowledge Fran Rogomentich for his work in the initial data acquisition phase of this project. This project has been supported in part by the NSF and the University of Connecticut Research Foundation.

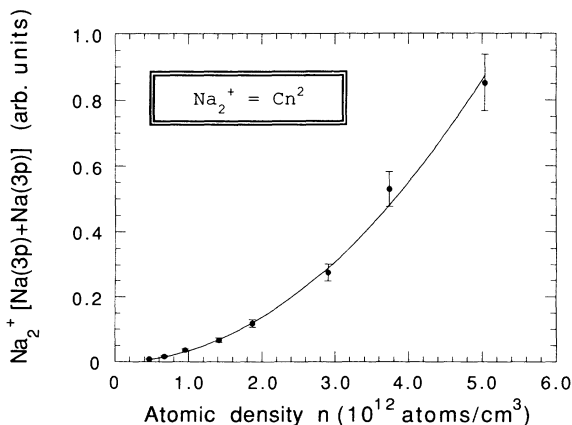


FIG. 7. Na_2^+ [associative ionization of $\text{Na}(3p)$] ion yield vs atomic density.

- [1] J. Huennekens and A. Gallagher, *Phys. Rev. A* **28**, 1276 (1983).
- [2] R. Bonanno, J. Boulmer, and J. Weiner, *Comments At. Mol. Phys.* **16**, 109 (1985); H. R. Thorsheim, Y. Wang, and J. Weiner, *Phys. Rev. A* **41**, 2873 (1990).
- [3] H. A. J. Meijer, *Z. Phys. D* **17**, 257 (1990); see also the review by A. N. Klucharev and V. Vujnovic, *Phys. Rep.* **185**, 55 (1990).
- [4] P. L. Gould, P. D. Lett, P. S. Julienne, W. D. Phillips, H. R. Thorsheim, and J. Weiner, *Phys. Rev. Lett.* **60**, 788 (1988).
- [5] Fran Rogomentich, M.S. thesis, University of Connecticut, 1987.
- [6] C. Gabbanini, M. Biagini, S. Gozzini, L. Lucchesini, and L. Moi, *J. Phys. B* **24**, 3807 (1991).
- [7] The Langevin model has long been used to calculate the mobility of atomic or molecular ions drifting in a neutral (unexcited) background gas: see, e.g., E. W. McDaniel, *Collision Phenomena in Ionized Gases*, 1st ed. (Wiley, New York, 1964), Appendix II.
- [8] The Na(3s) ground-state polarizability has been measured as $20(2.5) \times 10^{-24} \text{ cm}^3$ [A. Salop, E. Pollack, and B. Bederson, *Phys. Rev.* **124**, 1431 (1961)], or $0.18n^6 a_0^3$. The Na(3p) scalar polarizability (which dominates over the tensor polarizability) is measured as $0.089 \text{ MHz}/(\text{kV}/\text{cm})^2 = 0.490n^6 a_0^3$ [R. W. Schmieder, A. Lurio, and W. Happer, *Phys. Rev. A* **3**, 1209 (1971)].
- [9] For a pedagogical discussion, see L. Landau and E. Lifshitz, *Mechanics* (Pergamon, London, 1960), p. 51.
- [10] D. Lubman, C. Rettner, and R. Zare, *J. Phys. Chem.* **86**, 1129 (1982).
- [11] W. E. Baylis, *Can. J. Phys.* **55**, 1924 (1977).
- [12] J. Nijland, J. deGouw, C. Uiterwaal, H. Dijkerman, and H. Heideman, *J. Phys. B* **23**, L553 (1990); see also O. Dulieu, A. Giusti-Suzor, and F. Masnou-Seeuws, *J. Phys. B* **24**, 4391 (1991).
- [13] H. Dengel, M.-W. Ruf, and H. Hotop, *Europhys. Lett.* **23**, 567 (1993).
- [14] C. J. Cerjan, K. K. Docken, and A. Dalgarno, *Chem. Phys. Lett.* **38**, 401 (1976); **40**, 205 (1976); A. Henriët and F. Masnou-Seeuws, *ibid.* **101**, 535 (1983).
- [15] D. E. Nitz, P. B. Hogan, L. D. Schearer, and S. J. Smith, *J. Phys. B* **12**, L103 (1979).
- [16] M. Allegrini, W. P. Garver, V. S. Kushawaha, and J. J. Leventhal, in *Collisions and Half-Collisions with Lasers*, edited by N. K. Rahman and C. Guidotti (Harwood Academic, New York, 1984), p. 109.
- [17] M. Svalgaard, Niels Bohr Institute, Research Report, University of Copenhagen, 1993 (unpublished); M. Svalgaard (private communication); C. Monroe (private communication).
- [18] C. Tapalian and W. W. Smith, *Chem. Phys. Lett.* **211**, 425 (1993).

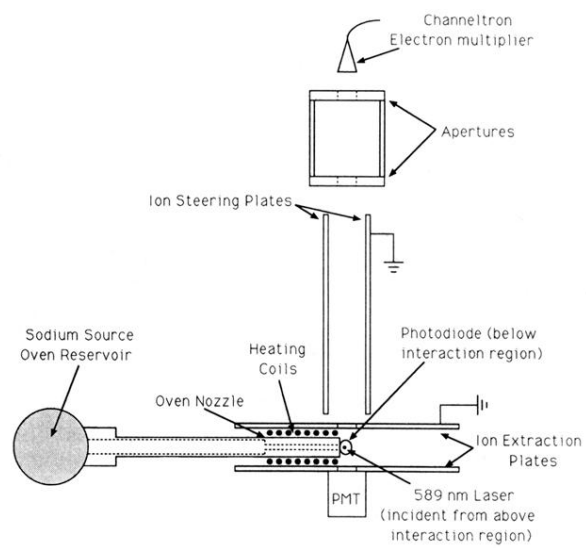


FIG. 2. Schematic diagram of time-of-flight atomic beam apparatus.

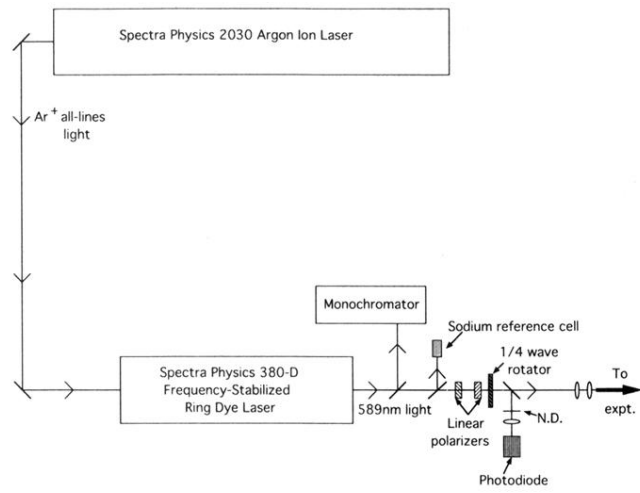


FIG. 3. Lasers and optical components. N.D. denotes a neutral-density filter.